

Band-Structure Engineering of Gold Atomic Wires on Silicon by Controlled Doping

Won Hoon Choi, Pil Gyu Kang, Kyung Deuk Ryang, and Han Woong Yeom*

Institute of Physics and Applied Physics and Center for Atomic Wires and Layers, Yonsei University, Seoul 120-749, Korea

(Received 12 July 2007; published 24 March 2008)

We report on the systematic tuning of the electronic band structure of atomic wires by controlling the density of impurity atoms. The atomic wires are self-assembled on Si(111) by substitutional gold adsorbates and extra silicon atoms are deposited as the impurity dopants. The one-dimensional electronic band of gold atomic wires, measured by angle-resolved photoemission, changes from a fully metallic to semiconducting one with its band gap increasing above 0.3 eV along with an energy shift as a linear function of the Si dopant density. The gap opening mechanism is suggested to be related to the ordering of the impurities.

DOI: [10.1103/PhysRevLett.100.126801](https://doi.org/10.1103/PhysRevLett.100.126801)

PACS numbers: 73.20.At, 68.43.Hn, 79.60.Dp

Recent progress on nanowire materials has provided a major practical solution in nanoscale electronic and biochemical device fabrication [1,2]. An essential step toward more versatile devices using nanowires is the systematic control of electronic properties through, for example, doping impurities. Indeed, the drastic changes of electronic properties of carbon nanotubes [3,4] and semiconductor nanowires [5–7] by atomic or molecular doping were recently demonstrated. However, the systematic control over the dopant density and the continuous and reproducible tuning of the electronic properties have been key technological issues in not only nanowire applications but also in various nanomaterials systems. The systematic doping becomes even more challenging when the host structures shrink down to a truly molecular or atomic scale due to fundamental reasons [8,9].

Here, we show the successful doping of atomic-scale gold wires (~ 1 nm in width), which are self-assembled on a silicon surface, by controlling the impurity density. A few well-ordered atomic wire arrays with metallic properties were reported recently on various silicon surfaces. These systems have one-dimensional (1D) metallic band structures and interesting 1D physics like Peierl's transitions and charge-density-wave ground states [10–12]. Among them, the gold atomic wires on a Si(111) surface, the Si(111)-(5 \times 2)-Au surface [13–17], were shown to host silicon adatoms and the possibility of their doping action, electron donation to gold wires, was theoretically proposed [15]. A successful density control of the silicon adatoms, here, indeed leads to the systematic tuning of the 1D band structure of gold atomic wires from a metal to a semiconductor with a linearly tunable band gap.

Microscopic studies were performed with a commercial variable-temperature scanning tunneling microscope (STM) (Omicron, Germany). The electronic band dispersions were measured by angle-resolved photoemission (ARP) employing monochromatized He discharge radiation ($h\nu = 40.2$ eV). The angular and energy resolution of the instrument is 0.15° and 15 meV. All STM and ARP measurements were performed at room temperature. LEED optics were available for both systems, which

were used not only to check the surface order but also to ensure the consistent surfaces in different experiments. The Si(111) substrate with a low n-type doping ($10 \Omega \text{ cm}$) was flash heated to produce a clean 7×7 reconstructed surface. A slightly miscut ($\sim 2^\circ$) substrate was used to make the terraces narrow (≤ 100 nm) [18], which forces the uniquely oriented growth of the gold atomic wires along the step edges. By depositing submonolayer of gold at 833 K, a well-ordered Si(111)-(5 \times 2)-Au surface was prepared on the substrate.

Figure 1 shows the STM image of the gold atomic wires and the corresponding structure model [15]. Each wire is composed of a double atomic chain of gold [bright (yellow contrast) stripes in Fig. 1(a)] embedded into the topmost silicon layer. The width of a wire is about 0.7 nm as separated with an interwire distance of 1.7 nm by silicon honeycomb chains. A characteristic feature of this system is that parts of the silicon surface atoms [protrusions in Fig. 1(a)] replaced by gold are randomly adsorbed on the wires, between two gold chains. The silicon adatoms have a unique adsorption site and a tendency to form their own chain with a $4a_{\text{Si}}$ [a_{Si} the lattice constant of Si(111) of 0.384 nm] spacing along the wire [13,14,17,19]. The density of Si adatoms is roughly reproducible in typical growth conditions as ~ 0.025 monolayer [14,19]. This corresponds to the 43%–48% occupation of all $4a_{\text{Si}}$ sites along the wires, as shown in Fig. 2(c).

In order to control the density of silicon adatoms, we first evaporate silicon onto the gold wire array. With the deposition of a proper amount and the annealing at an optimized temperature of 423 K, the silicon adatom density can be increased to almost 100% (~ 0.05 monolayer) of all available sites [Fig. 2(a)] [19]. The clustering of Si adatoms [larger spots in Fig. 2(a)] starts at this density. We call this the adatom-saturated wire. The adatom density, then, can be reduced by further annealing above ~ 400 K to sublimate the silicon adatoms; a higher temperature for a lower density. The adatom density is counted from the STM images taken after each annealing. The annealing temperature vs adatom density relationship can reliably be established through repeated deposition-annealing cycles.

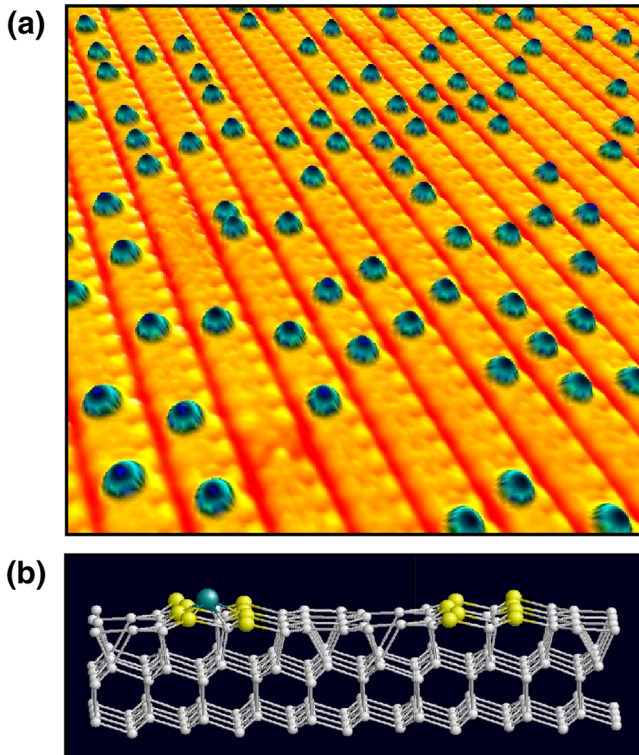


FIG. 1 (color online). (a) STM image of the gold atomic wire array formed on Si(111) with silicon adatoms (in blue contrast) and (b) its atomic structure model [15]; gray (small), yellow (medium), and blue (large) balls represent substrate silicon atoms, gold atoms, and silicon adatoms, respectively.

This stepwise annealing sequence almost saturates at about 870 K with the adatom density reduced to about 48%, back to the as-grown wires. A further reduction of the density, down to 36.8%, [Fig. 2(d)] can only be achieved by a flash annealing to a much higher temperature of 1173 K. The host wire structure is quite robust during these procedures as no significant change of the local structure is noticed in STM while the defect density gradually increases for repeated cycles. In order to minimize the influence of such defects, the fresh Si(111)-(5 × 2)-Au surface is prepared for each deposition-annealing cycle.

The density of the silicon adatoms controls the electronic structure systematically. Figure 3 is the ARP spectra near the Fermi level taken up to the emission angle of 35° along the wires with a minimum adatom density of 36.8% [Fig. 3(a)] and the adatom-saturated one [Fig. 3(b)]. The minimally doped wires have three 1D bands, tagged as $S1$, $S2$, and $S3$ in Fig. 3(c) [15]. The $S3$ band has a sine-wave-like dispersion and is insulating. Another fully occupied band $S1$ is very weak and shallow near the Fermi level with only a marginal dispersion. The most important band is $S2$ which has a sharp parabolic dispersion to cross the Fermi level at the momentum (k_{\parallel}) of 0.57 \AA^{-1} . This 1D band has an effective mass of only a quarter of the free electron mass and the band filling of 0.3, between $1/3$ and $1/4$. That is,

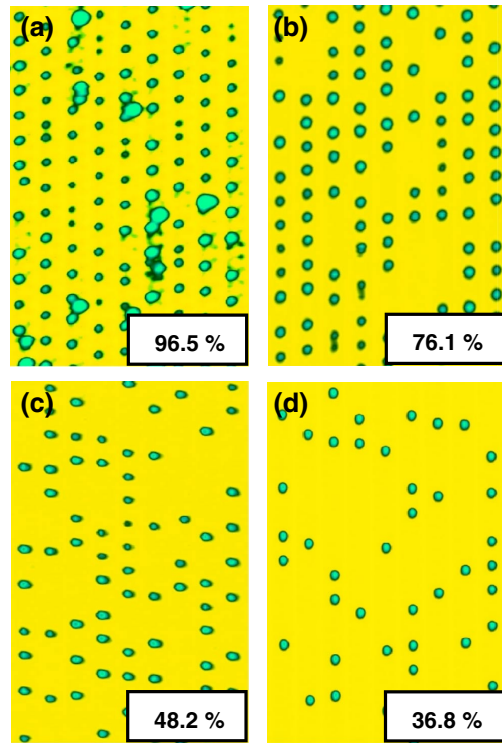


FIG. 2 (color online). STM images, with oversimplified contrast, for the gold wire array after the deposition of silicon (appearing as protrusions) with postannealings at different temperatures. The silicon adatoms tend to form rather regular $4a_{\text{Si}}$ -spaced chains at high density and the “saturation” of all $4a_{\text{Si}}$ -spaced sites along the wires is defined as 100% density. The Si density is systematically controllable from about 97% (a) down to 48% (c) by increasing the annealing temperature from 423 to 833 K and further down to 36% (d), which is called as the “minimally-doped” wires, by higher temperature flash annealing.

the $S2$ band is metallic with its electrons fully delocalized to make the wires good 1D conduction channels. This kind of fractionally filled 1D bands is commonly observed for various gold atomic wires on different silicon surfaces such as Si(110), Si(553), Si(557), and Si(5512) [11,12,20–22]. The microscopic origin of the $S1$ - $S3$ bands is not fully understood since the present structure model [15] only partly explains the band structure. The theoretical model for the undoped gold wires reproduce well the dispersions of the insulating $S1$ and $S3$ bands [thin solid lines in Fig. 3(c)] but not that of the—most important—metallic $S2$ band. This may be due to the limitation of the structure model itself as recently pointed out [13] or due to the fact that the experimental result is not for the completely undoped wires but for the silicon adatom density of at least 0.018 monolayer.

Figure 4 shows the change of the band dispersions near the Fermi level at different silicon adatom density. As the adatom density increases from the minimally-doped one,

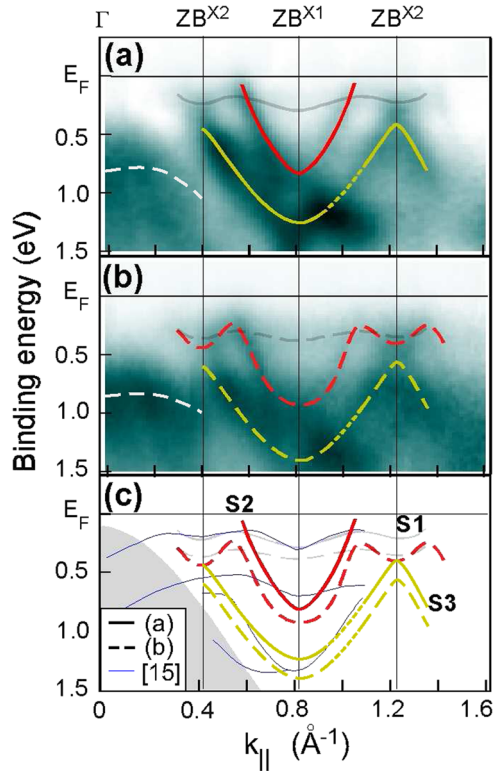


FIG. 3 (color online). Electron-energy-band dispersions along the gold wires measured with angle-resolved photoemission. (a) The minimally doped wires with a metallic band (S2) and (b) those with saturated silicon adatoms with a fully opened band gap (0.3 eV below the Fermi level). The dispersion curves in solid or dashed lines are guides for the spectral features with high intensity within an accuracy of roughly 50 meV but are not decisive for the dotted parts due to the weak intensity and the interference with an extra surface state not mentioned here [15]. (c) The comparison of the measured band dispersions with those of the theoretical calculation for undoped wires [15]. The boundaries of $\times 1$ ($ZB^{\times 1}$) and $\times 2$ ($ZB^{\times 2}$) Brillouin zones are shown. The white dashed lines in (a) and (b) indicate the bulk-band spectral feature.

the S2 band gradually shifts to a higher binding energy, loses its intensity near the Fermi level, and finally folds back toward the $\times 2$ Brillouin zone boundary ($ZB^{\times 2}$ at $k_{\parallel} \sim 0.4 \text{ \AA}^{-1}$). The overall downward energy shift ($0.23 \text{ eV} \pm 0.03 \text{ eV}$) is also rigidly observed for S1 and S3. The gradual band-gap opening at the Fermi level is shown clearly in the energy distribution curves of photoelectrons of Fig. 4(b). The evolution of the band gap is quantified by the leading-edge shifts of the energy distribution curves [11,12] as summarized in Fig. 4(c). It clearly indicates that the band gap increases as a function of the adatom density. The top of the S2 band at the adatom-saturated wires is located at $0.30 \pm 0.03 \text{ eV}$ below the Fermi level (the leading-edge shift of 0.16 eV) [23]. If we assume that the band gap is symmetric as centered on the Fermi level, this corresponds to a full band-gap size of

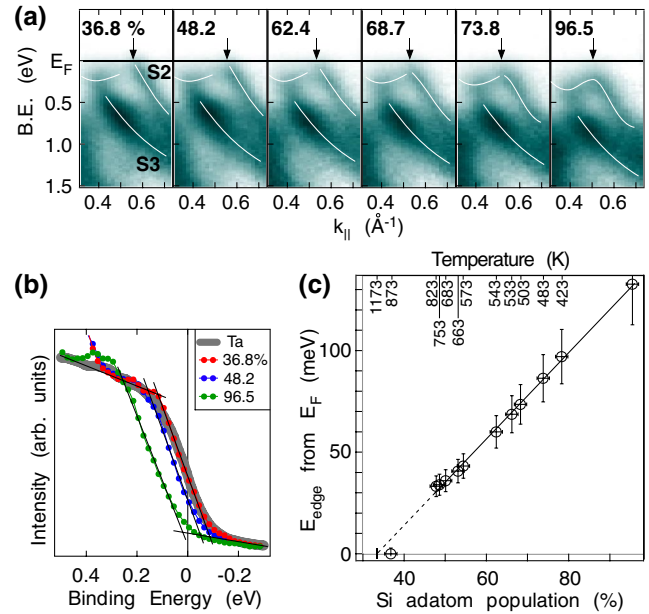


FIG. 4 (color online). (a) Evolution of the band structure near the Fermi level as increasing the density of silicon adatoms. The data were taken for the electron emission angle of $6^\circ - 14^\circ$ along the wires. (b) The energy distribution curves for the photoelectrons around the Fermi level for a few adatom densities showing clearly the evolution of the band gap, which is quantified by the simple linear fit (straight solid lines overlaid) of the leading edge. A similar curve for a tantalum metal (gray) is given to confirm the fully metallic character (the null band gap) of the minimally doped wires (red, 36.8%). (c) The measured band-gap size below the Fermi level [23] as a function of the adatom density (or the postannealing temperature after silicon deposition). The arrows in (a) indicate the Fermi momentum or the positions of the top of the bands for metallic or gapped bands, respectively.

0.6 eV. Even though the band gap opens asymmetrically, the final gap size should be larger than 0.3 eV. Consequently, we are able to convert the metallic gold atomic wires into a semiconducting ones and, moreover, to tune the band gap continuously from 0 to above 0.3 eV through doping the wires by silicon adatoms. Note that this process, saturating silicon adatom and reducing its density, is fully reproducible and reversible.

This band-structure change, especially the band-gap opening, rejects a few simple interpretations of the underlying mechanism. First, the present case is largely different from the conventional doping of semiconductor crystals, where the Fermi level position changes within a fixed band gap (or the rigid shift of the bands). Second, the typical doping of a metallic system simply increases the occupation of metallic electrons, that is, shifts the metallic electron band to higher binding energy without opening a band gap. Such a behavior was well established for the prototype 2D metallic system formed on a Si(111) surface, the Si(111)-Ag surface [24]. In the case of a molecular level

structure, such as a single C_{60} molecule, the doped electrons fill lowest-unoccupied-molecular levels to shift the whole energy levels rigidly [25].

From the above discussion, one can realize that at least the overall shift of the $S1$ - $S3$ bands near the Fermi level must be understood from the conventional action of the doped electrons, filling the $S2$ band gradually. No similar energy shift is found for the bulk bands (shown partly in Fig. 3) excluding the possibility of artifacts such as the surface photovoltage effect. Moreover, the partial electron transfer from the silicon adatoms into the gold wires was predicted by the theory [15]. However, in order to explain the band-gap opening, another mechanism is needed. It should also be mentioned that the present gap opening cannot be explained by the disorder driven metal-insulator transition, or localization transition, since the surface ordering, in fact, increases at high adatom density over 50%, where the band gap increases.

As a contrasting mechanism to the adatom-induced disorder, we suggest that the band gap is formed by the $4a_{Si}$ ordering of the adatoms. As seen in the STM images of Fig. 2, the $4a_{Si}$ ordering (or an extra $4a_{Si}$ lattice/ion potential for the 1D electrons of the gold wires) becomes stronger as the adatom density increases. This partial order is not clear in LEED but confirmed in the Fourier transformation of the STM images. This potential can drive the bands to form a gap around $1/4$ of the Brillouin zone, the corresponding momentum space point of the $4a_{Si}$ order, which is incidentally very close to the Fermi level crossing of the $S2$ band. Then, the increasing band gap can naturally be explained by the enhancing $4a_{Si}$ potential at a higher coverage and by the overall shift of Fermi level position within the gap due to the electron doping.

In support of this idea, the recent scanning tunneling spectroscopy study [26] reported that the short silicon adatom chains with a local $4a_{Si}$ ordering make those wire segments locally insulating. The maximum local band-gap size measured is 0.6 eV in qualitative accord with the band gap observed here for the adatom-saturated wires. That is, the band-gap opening is not due to individual adatoms but there is a novel collective mechanism by locally ordered adatom clusters.

A few complications, however, remain unsolved to invite further studies. First, the present band-structure measurement reveals well-defined bands without any sign of a mixture of metallic and insulating domains throughout the whole dopant density in contrast to the nanoscale inhomogeneity observed by local spectroscopy [27]. A similar inconsistency between the microscopic inhomogeneity and the global electronic states was recently pointed out for the high-temperature superconductors with inhomogeneous doping profiles [28,29]. Second, the band-gap position observed here slightly deviates from $1/4$ of the Brillouin zone. Although the reason for this discrepancy is not clear, it is apparent that the electronic energy gain is

maximized not by the gap formation at $1/4$ of the Brillouin zone with the gap located below the Fermi level but by the band-gap opening at the Fermi level, as observed here.

This work was supported by the CRi program of MOST of Korea through Center for Atomic Wires and Layers.

*yeom@yonsei.ac.kr

- [1] A. H. Flood, J. F. Stoddart, D. W. Steuerman, and J. R. Heath, *Science* **306**, 2055 (2004).
- [2] Z. Chen *et al.*, *Science* **311**, 1735 (2006).
- [3] K. Kamaras, M. E. Itkis, H. Hu, B. Zhao, and R. C. Haddon, *Science* **301**, 1501 (2003).
- [4] C. Zhou, J. Kong, E. Yenilmez, and H. Dai, *Science* **290**, 1552 (2000).
- [5] Y. Wu, J. Xiang, C. Yang, W. Lu, and C. M. Lieber, *Nature (London)* **430**, 61 (2004).
- [6] J. Bettini *et al.*, *Nature Nanotechnology* **1**, 182 (2006).
- [7] Y. Cui, X. Duan, J. Hu, and C. M. Lieber, *J. Phys. Chem. B* **104**, 5213 (2000).
- [8] G. M. Dalpian and J. R. Chelikowsky, *Phys. Rev. Lett.* **96**, 226802 (2006).
- [9] S. C. Erwin *et al.*, *Nature (London)* **436**, 91 (2005).
- [10] H. W. Yeom *et al.*, *Phys. Rev. Lett.* **82**, 4898 (1999).
- [11] J. R. Ahn, H. W. Yeom, H. S. Yoon, and I. W. Lyo, *Phys. Rev. Lett.* **91**, 196403 (2003).
- [12] J. R. Ahn, P. G. Kang, K. D. Ryang, and H. W. Yeom, *Phys. Rev. Lett.* **95**, 196402 (2005); P. C. Snijders, S. Rogge, and H. H. Weitering, *ibid.* **96**, 076801 (2006).
- [13] H. S. Yoon, J. E. Lee, S. J. Park, I. W. Lyo, and M. H. Kang, *Phys. Rev. B* **72**, 155443 (2005) and references therein.
- [14] A. Kirakosian, R. Bennewitz, F. J. Himpsel, and L. W. Bruch, *Phys. Rev. B* **67**, 205412 (2003).
- [15] S. C. Erwin, *Phys. Rev. Lett.* **91**, 206101 (2003).
- [16] M. H. Kang and J. Y. Lee, *Surf. Sci.* **531**, 1 (2003).
- [17] R. Losio, K. N. Altmann, and F. J. Himpsel, *Phys. Rev. Lett.* **85**, 808 (2000).
- [18] J.-L. Lin *et al.*, *J. Appl. Phys.* **84**, 255 (1998).
- [19] R. Bennewitz *et al.*, *Nanotechnology* **13**, 499 (2002).
- [20] J. N. Crain *et al.*, *Phys. Rev. Lett.* **90**, 176805 (2003).
- [21] J. L. McChesney, J. N. Crain, F. J. Himpsel, and R. Bennewitz, *Phys. Rev. B* **72**, 035446 (2005).
- [22] J. R. Ahn, H. W. Yeom, E. S. Cho, and C. Y. Park, *Phys. Rev. B* **69**, 233311 (2004).
- [23] The quantification of a band gap by leading-edge shifts tends to underestimate the gap size. For a fully developed band gap with well-defined quasiparticle peaks, the gap size can be determined accurately from the position of the top of the band.
- [24] J. N. Crain, M. C. Gallagher, J. L. McChesney, M. Bissen, and F. J. Himpsel, *Phys. Rev. B* **72**, 045312 (2005); I. Matsuda *et al.*, *Phys. Rev. B* **71**, 235315 (2005).
- [25] R. Yamachika, M. Grobis, A. Wachowiak, and M. F. Crommie, *Science* **304**, 281 (2004).
- [26] H. S. Yoon, S. J. Park, J. E. Lee, C. N. Whang, and I.-W. Lyo, *Phys. Rev. Lett.* **92**, 096801 (2004).
- [27] J. L. McChesney *et al.*, *Phys. Rev. B* **70**, 195430 (2004).
- [28] K. McElroy *et al.*, *Science* **309**, 1048 (2005).
- [29] M. Vershinin *et al.*, *Science* **303**, 1995 (2004).